ELSEVIER

Journal of Nuclear Materials 241–243 (1997) 777–781

journal of nuclear materials

Screening of recycling and non-recycling impurities in the Alcator C-Mod tokamak

G.M. McCracken [a,*], R.S. Granetz [a], B. Lipschultz [a], B. LaBombard [a], F. Bombarda [b], J.A. Goetz [a], S. Lisgo [c], D. Jablonski [a], H. Ohkawa [a], J.E. Rice [a], P.C. Stangeby [c], J.L. Terry [a], Y. Wang [a]

[a] *Plasma Fusion Center, Massachusetts Institute of Technology, Cambridge, MA 02139, USA*
[b] *Associazione EURATOM-ENEA sulla Fusione, 00044 Frascati, Italy*
[c] *Institute of Aerospace Studies, University of Toronto, Toronto, Ont., Canada M3H 5T6*

Abstract

The behavior of argon and nitrogen, injected into single null diverted Ohmic discharges, has been compared. The screening of the divertor and scrape-off layer plasma is studied by comparing the number of impurity atoms in the core with the number injected by a calibrated gas puff. The effect of the poloidal position of injection on screening has been investigated. The core nitrogen density is dependent of an poloidal position of injection while the argon density is not. The spatial distribution of low charge states in the divertor has also been studied using a multichord visible spectrometer. Initial results of nitrogen modeling with the Monte Carlo code DIVIMP are presented.

Keywords: Alcator C-Mod; Tokamak; Impurity transport; Poloidal divertor

1. Introduction

One of the principal functions of a divertor is the removal of the plasma material interaction to a remote location where the impurities produced have a small probability of reaching the confined plasma and polluting it. The divertor can reduce impurities in two ways, firstly, by establishing a plasma temperature gradient between the confined plasma and the divertor target which reduces the impurity sputter yield and, secondly, by screening i.e. reducing the probability of impurities produced at the target reaching the confined plasma [1,2]. Screening may occur by competition between parallel and cross-field transport. A high ionization rate in the SOL, far from the separatrix, is generally likely to improve the screening since it will decrease the cross-field diffusion rate into the core. However there are parallel temperature gradient forces which can push the impurity ions towards the confinement region. Good screening depends on having the parallel force due to the friction of the plasma flowing towards the target greater than the ion temperature gradient force acting away from it [3,4].

The screening process in the SOL of the high density tokamak, Alcator C-Mod [5] has been studied using gaseous impurities. Gas puffing has the advantage of giving independent control of the impurity injection rate under a range of operating conditions so that the screening process can be studied independently of the impurity production process. In the present paper the effect of different poloidal injection positions on the screening of impurities has been extensively studied.

Impurity behavior can be broadly classified as either recycling or non-recycling. The rare gases He, Ne and Ar are typical recycling species. Since they are chemically inert, ions arriving at a surface are backscattered with some fraction of their thermal energy plus the energy acquired in the plasma sheath potential at the target. After recycling they may therefore penetrate deeply into the plasma before ionization. Non-recycling impurities are typ-

* Corresponding author. Presently at: JET Joint Undertaking, Abingdon, OX14 3EA, UK. Tel.: +44-1235 46 50632; fax: +44-1235 46 5063; e-mail: garry.mccracken@jet.uk.

0022-3115/97/$17.00 Copyright © 1997 Elsevier Science B.V. All rights reserved.
PII S0022-3115(96)00605-8

ified by carbon and metals which are expected to have a low back-scattering probability. Somewhat surprisingly it has been found that nitrogen gas also acts like a non-recycling impurity [6], presumably due to its chemical interaction with solid surfaces.

2. Experiment

Screening experiments have been carried out using a number of gases: He, Ne, Ar, CD_4 and N_2. In the present study we concentrate on Ar and N_2. The details of much of the experimental arrangement have been described previously [7,8]. The gas is injected through a number of capillary tubes entering the vessel at different poloidal and toroidal locations, A to G, Fig. 1. In addition there is a single piezo valve, H, at the outer wall which is used to obtain a faster time response than the capillaries. The nitrogen radiation in the core plasma is measured with a single spatial channel, scannable VUV spectrometer [9] and the argon with a crystal spectrometer [10] viewing Ar XVII at up to 5 chords simultaneously. The MIST code [11] is used to calculate the charge state distribution, including transport, and hence the total impurity content. The code results are calibrated by the measured brightness of the Ar XVII or N VII.

The impurity flux from the divertor surfaces is monitored with a visible spectrometer using a 2D CCD detector. A wavelength range of up to 45 (70) nm can be scanned in 45 ms with a spectral resolution of 0.1 (0.15) nm. Optical fibers view up to 14 locations at both the inner and outer divertor simultaneously (see Fig. 1). In addition, there are

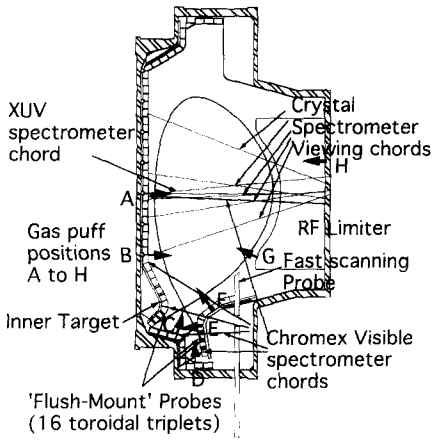

Fig. 1. Poloidal cross-section of Alcator C-Mod showing the gas puffing positions, A to H. (A) Inner midplane. (B) Inner lower wall. (C) Private flux zone. (D) Divertor slot. (E) Lower outer target. (F) Upper outer target. (G) Outer RF limiter. (H) Outer midplane. The position of the Langmuir probes in the divertor and SOL and the spectroscopic views of the VUV spectrometer, the crystal spectrometer and the visible spectrometer are also shown.

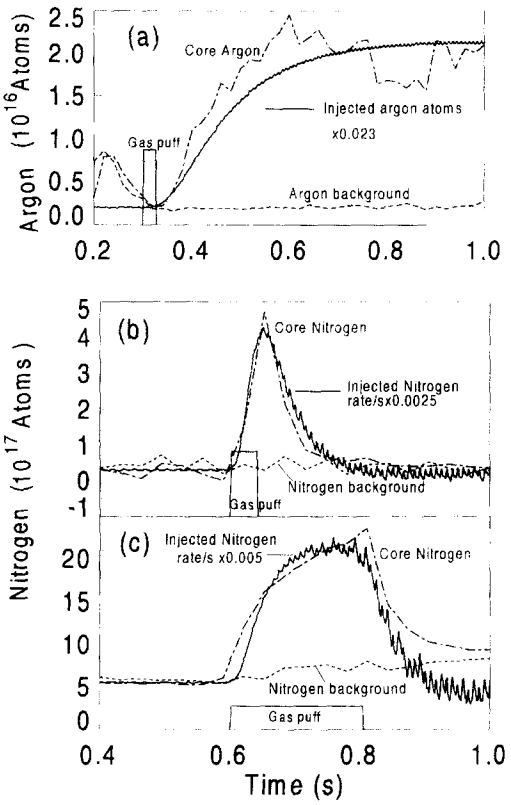

Fig. 2. Comparison of the time behavior of argon (a) and nitrogen (b) injected in a short pulse from position H, Fig. 1. (c) Time behavior of a longer pulse of nitrogen injection. In (a) the number of confined Ar atoms is compared with the integrated number injected from a gas injection calibration. In (b) and (c) the normalized injection rate of nitrogen is used for comparison.

core measurements of n_e, T_e, total radiation profiles, Z_{eff} and other spectroscopic diagnostics. The n_e and T_e profiles in the SOL and at the target plates are measured with a scanning probe and an array of Langmuir probes in the tiles, respectively [12]. The impurity injection experiments have been carried out both under conditions where the effect on plasma parameters is small and also where the injection of the impurity has been a serious disturbance, causing the plasma to detach from the divertor target [13]. Typical conditions at the divertor plate vary from $T_e = 20$ eV, $n_e = 1 \times 10^{19}$ m^{-3} for the non-perturbative studies to $T_e = 2$ eV, $n_e = 2 \times 10^{20}$ m^{-3} for the detached conditions.

3. Results

3.1. Argon

For low gas injection rates the number of argon atoms inside the separatrix at any given time during the discharge

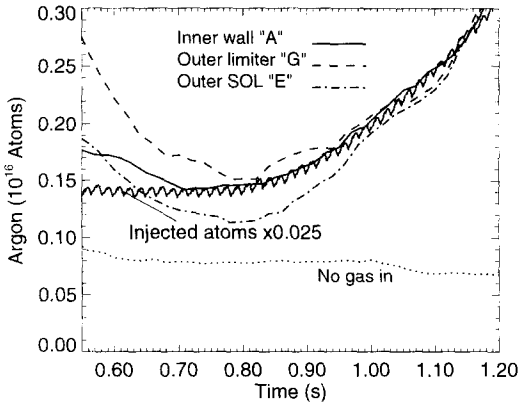

Fig. 3. The time behavior of the core argon when argon gas is injected at 3 different poloidal positions, Inside midplane (A), outside limiter (G) and outer SOL (E). The amount of argon injected, obtained from a calibration pulse $\times 0.025$, is shown for comparison.

is proportional to the total number injected, Fig. 2a. The number of Ar atoms injected, obtained from the pressure rise in the vacuum vessel during a calibration pulse, has also been plotted, normalized to the number in the plasma. Approximately 2% of the injected atoms are in the confined plasma. Gas has also been injected via the capillary tubes into the private flux zone in the divertor, at the inner wall midplane and into the outer SOL (positions A, E and G, Fig. 1). The number of atoms in the core is compared with the number of atoms injected in Fig. 3. Typically 3% of the injected atoms are in the confined plasma. It is seen that within the scatter in the data the number of confined atoms is independent of the gas puffing position. The fraction of argon getting into the confined plasma is a decreasing function of density as previously reported [7] varying from 3% down to 0.7% as the density $\bar{n}_e$ increases from 1 to 3×10^{20}. A number of studies of the dependence on divertor geometry has been carried out [14]. In general there is little effect due to the plasma configuration. Variation of the outer gap from 6.5 to 23 mm, of the elongation κ, from 0.9 to 1.4 and varying the position of the strike point on the vertical targets made less than 25% variation in the screening, with no consistent trends. These results for diverted plasmas contrast with those obtained when argon is puffed into similar limiter discharges. As much as 45% of the injected atoms then appear in the confined plasma and the number is dependent on the poloidal position of injection [15].

3.2. Nitrogen

In contrast to the rare gases, nitrogen or methane puffs result in an impurity concentration in the confined plasma which decays with a time constant of ~ 30 ms at the end of the injection pulse, Fig. 2b, c. The time constant is comparable to that measured for impurities injected by laser ablation (typically scandium) and indicates an impurity recycling coefficient < 0.3. For a long impurity injection pulse the impurity concentration rises to a constant value, Fig. 2c. It is observed in both Fig. 2b, c that the total number of impurities in the plasma is proportional to the impurity injection rate (obtained from the gas calibration) over the whole injection cycle, rather than being proportional to the integrated amount, as is the case for argon. The penetration factor (PF), defined as the impurity number in the confined plasma normalized to the influx [16], is a characteristic time which varies from 10^{-4} to 10^{-2} s, depending on species and conditions.

Using a fixed nitrogen injection pulse the effect of varying the plasma density in Ohmic diverted discharges has been investigated. It is found that penetration factor decreases slowly with increasing density in a similar way to argon. However at densities above about $\bar{n}_e = 1.8 \times 10^{20}$ m^{-3} the plasma detaches at the outer target. This leads to an increase in the nitrogen density in the core as shown in Fig. 4, where detachment occurred at 0.81 s. The detachment is shown clearly by the drop in plasma temperature at the outer divertor target. As the core confinement does not change significantly during divertor detachment the change in penetration factor is attributed to changes in the divertor plasma conditions.

The effect of varying the poloidal position of the injected impurity has been studied. The results for attached plasmas in Ohmic discharges are shown in Fig. 5. Because the plasma detaches even without impurity injection at

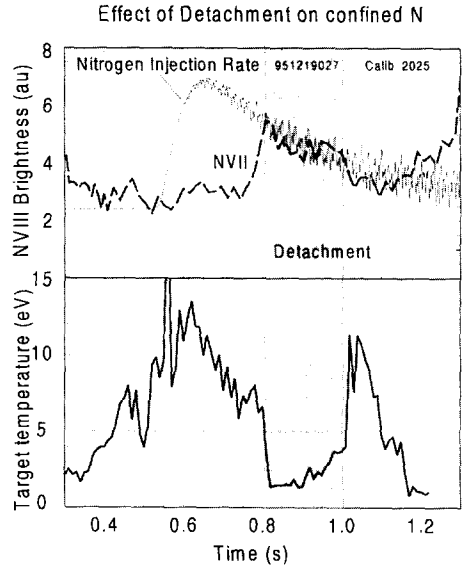

Fig. 4. The effect of detachment on the nitrogen core density. (a) The relative N density from the N VII brightness. (b) The plasma temperature T_e from a probe close to the strike point on the outer target.

$\bar{n}_e = 1.8$ to 2×10^{20} m^{-3}, measurements in attached plasmas can only be made over a limited range of densities. It is observed that the best screening for attached plasmas appears to be for gas injection at the inner wall, with least good screening at the outer midplane. As in the case of the recycling gases, screening is better at higher densities.

3.3. Divertor spectroscopy

In order to follow the transport of the injected impurities the spatial distribution of the visible impurity radiation in the divertor has been studied using a multi-channel visible spectrometer with chords spanning the inner and outer divertor. The charge states NI (868.0), NII (463.0 nm), NIII (451.5 nm) and ArII (442.6 nm) have been examined. In attached discharges the H_α and the total radiation are significantly larger at the inner than the outer divertor target [17], which is consistent with the lower value of T_e there [12]. It is thus expected that the impurity radiation will be largest at the inner target also.

The spatial distribution of the line brightness of NII and NIII, with different viewing chords during N_2 gas injection from the inner wall, is shown in Fig. 6 for attached plasmas. The behavior of NII and NIII is similar with the brightness of both charge states being peaked just above the inner strike point, near the inner divertor 'nose'. During detachment the brightness drops and the peak intensity moves up ~ 10 mm spatially. Even in attached conditions the NI intensity does not increase above the background when the N_2 is injected. The brightness of the NIII decreases at all locations with increasing $\bar{n}_e$ over the range 1.3 to 2.8×10^{20} m^{-3}, in some cases by as much as a factor of more than 10. The impurity fluxes have not yet been calculated from the chordal brightness because of uncertainty in the plasma density and temperature along the viewing chords and in the photon efficiencies of the nitrogen lines. However even the spatial distribution of the radiation is a useful check on models.

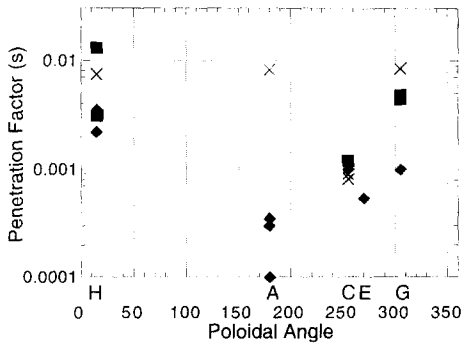

Fig. 5. Variation of the penetration factor of nitrogen for different poloidal injection positions in attached plasmas at different densities. The injection rate is in the range 2 to 4×10^{20} atoms s^{-1}. (■) $\bar{n}_e = 1.3$–1.5×10^{20} m^{-3}; (◆) $\bar{n}_e = 1.6$–1.9×10^{20} m^{-3}; (×) calculated value using DIVIMP, all experimental values of n_e.

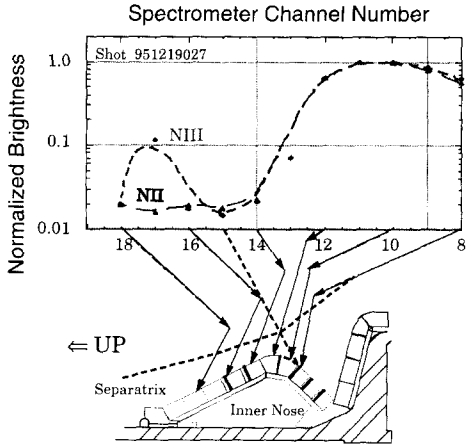

Fig. 6. The spatial distribution of the brightness of NII and NIII at the inner divertor target for attached divertor plasmas. Each charge state has been independently normalized. The orientation of the inner divertor can be seen more clearly in Fig. 1.

There is a problem that the background of the low ionization states builds up during an experimental run, from near the detectable limit to a value as much as 10 times higher. It is presumably due to the build up of the nitrogen on divertor target surfaces and its subsequent release by ion induced desorption, due to the plasma ion flux. This background decays by a factor of 2 in about 10 shots after nitrogen injection stops. An increased background nitrogen density in the core plasma is also observed.

4. Discussion

The differences between the argon and nitrogen are marked both in their time dependence and in their dependence on poloidal position of injection. Qualitatively, such differences are expected on the basis of the definition of recycling and non-recycling species. Multiple chances for re-entering the plasma allow recycling impurities to be redistributed poloidally and toroidally. It has been found that there is no dependence of the Ar core density on the poloidal position of injection. This is also true for deuterium in Alcator C-Mod. Further experiments are planned to see if impurities in the divertor can account for the large fraction of the total amount injected which is not in the core plasma.

The non-recycling species are interesting from a number of points of view. The intrinsic impurities (metals, carbon, boron), are of course non-recycling. Assuming that non-recycling species are ionized in the SOL, the single 'pass' through the plasma means that the impurity density in the SOL is expected to be proportional to the flow rate.

Since there are no recycling atoms no assumptions are required for the energy and angular distribution for these species.

Modeling has been started using the 2D Monte Carlo code, DIVIMP [18]. The experimental n_e and T_e profiles are used as input to an onion-skin model to calculate the n_e and T_e distribution in the SOL for each discharge. Results are compared to experimental data in Fig. 5. For a cross field diffusion coefficient $D = 1.0\ m^2\ s^{-1}$, agreement between model and experiment is within a factor of 2 except at the inner wall, location A, Fig. 1. Screening is better for atoms injected into the divertor than at the outer midplane. Less dependence on n_e is observed in the model than in the experiment. More notable is the large difference between the measured and modeled penetration factors when gas is injected from the inner wall. The low measured values are at first surprising. However since there is a complete toroidal sink at the inside wall, while the outer protection limiter is localized both toroidally and poloidally, the low PF may be due to the fact that ionization is taking place far from the separatrix and the ions are lost to the wall even before they get to the divertor. However direct observations of parallel flow towards the divertor target have consistently been made [19]. Further DIVIMP studies are planned to investigate these effects. In particular the calculated distribution of the low charge states in the divertor will be compared with experimental results. It is important to note that thermal gases do not penetrate as far into the plasma as sputtered atoms because of their lower energy: they will therefore be better screened. No direct measurement of the effect of higher energy species has yet been made on C-Mod.

5. Summary

There is good screening for both recycling and non-recycling gases in diverted Ohmic discharges; this is attributed to the high plasma density and high power density in the C-Mod SOL. The radial location of ionization is, in all cases, in the SOL. This is partly due to the low energy of the injected gas species. While the core density of a recycling species is proportional to the total number of injected atoms and is independent of the poloidal position of injection, the density of a non-recycling species is proportional to the rate of injection and is dependent on the injection position. The screening of both recycling and non-recycling species is significantly reduced when the plasma detaches from the divertor target.

Screening of non-recycling impurities is best when impurities are injected in the divertor or at the inner wall. The good screening at the inner wall is tentatively ascribed to the sink action of the toroidally continuous wall. Modeling with DIVIMP generally gives good agreement with experiment showing much better screening for impurities injected in the divertor than at the outer midplane. Spectroscopic measurements of the impurities in the divertor indicate that they are concentrated near the inner strike point.

Acknowledgements

The authors are grateful to the whole Alcator team and in particular to the operations group, for the excellent operation of the machine. This work is sponsored by the US Department of Energy under contract No. DE-AC02-78ET51013.

References

[1] P.C. Stangeby and G.M. McCracken, Nucl. Fusion 30 (1990) 122.
[2] C.S. Pitcher and P.C. Stangeby, Plasma Phys. Controlled Fusion, to be published.
[3] J. Neuhauser, W. Schneider, R. Wunderlich and K. Lackner, Nucl. Fusion 24 (1984) 39.
[4] J. Roth, K. Kreiger and G. Fussman, Nucl. Fusion 32 (1992) 1835.
[5] I.H. Hutchinson, R. Boivin, F. Bombarda et al., Phys. Plasmas 1 (1994) 1511.
[6] J.V. Hoffman, private communication, March (1995).
[7] G.M. McCracken, F. Bombarda, M. Graf et al., J. Nucl. Mater. 220–222 (1995) 264.
[8] G.M. McCracken, B. Lipschultz, B. LaBombard, Controlled Fusion and Plasma Physics, Proc. 22nd EPS, Bournemouth Vol. II (1995) p. 313.
[9] M.A. Graf, J.E. Rice, J.L. Terry et al., Rev. Sci. Instrum. 66 (1995) 636.
[10] J.E. Rice and E.S. Marmar, Rev. Sci. Instrum. 61 (1990) 2753.
[11] R.A. Hulse, Nuclear Technol./Fusion 3 (1983) 259.
[12] B. Labombard, J. Goetz, C. Kurz et al., Phys. Plasmas 2 (1995) 2242.
[13] B. Lipschultz, J. Goetz, B. Labombard et al., J. Nucl. Mater. 220–222 (1995) 50.
[14] Y. Wang, Ph.D., Thesis, Plasma Fusion Center MIT (1996).
[15] R.A. Granetz et al., these Proceedings, p. 788.
[16] G. Janeschitz, R. König, L. Lauro-Taroni et al., J. Nucl. Mater. 196–198 (1992) 380.
[17] J. Goetz, C. Kurz, B. Labombard et al., Phys. Plasmas 3 (1996) 1908.
[18] P.C. Stangeby and D. Elder, J. Nucl. Mater. 196–198 (1992) 258.
[19] D. Jablonski, B. LaBombard, B. Lipschultz et al., these Proceedings, p. 782.